

## Structural and Morphological Properties of Fe<sub>2</sub>O<sub>3</sub> and TiO<sub>2</sub>:Fe<sub>2</sub>O<sub>3</sub> Thin Films Prepared by Spray Pyrolysis Technique

\*Asia Hussein Kadhim

Nahida B. Hasan

Department of Physics, College of Science, University of Babylon, Iraq.

\*Corresponding Author E-mail: [asia.hu1974@gmail.com](mailto:asia.hu1974@gmail.com)

### ARTICLE INFO.:

Article history:

Received: 28 JUN, 2018

Accepted: 8 JUL, 2018

Available Online: 11 JUL, 2019

Keywords:

Iron oxide films

Spray pyrolysis

Structural properties

morphological Properties

### ABSTRACT:

Various doping percentage (1, 3 and 5 %) of titanium dioxide TiO<sub>2</sub> were successfully introduced into the iron oxide Fe<sub>2</sub>O<sub>3</sub> thin films obtained by spray pyrolysis technique (SPT) on a glass substrates. The effect of TiO<sub>2</sub> doping on structural and morphological properties of deposited thin films was studied by X-ray diffraction analysis and atomic forces microscope (AFM) respectively. XRD result showed that all samples are polycrystalline and the crystallite size decrease with increasing percentage of (TiO<sub>2</sub>). All films have peaks appears at (110), (211), (101), (222), (210), (202), (312), (332), (310) and (432) planes with preferred orientation along (211). The (AFM) results shows that the grain size, roughness rate and the root mean square decreases with increasing dopant ratios.

DIO.: <http://dx.doi.org/10.31257/2018/JKP/2019/110105>

الخصائص التركيبية والطوبوغرافية لأغشية Fe<sub>2</sub>O<sub>3</sub> و TiO<sub>2</sub>:Fe<sub>2</sub>O<sub>3</sub> الرقيقة المحضرة بطريقة الرش الكيميائي الحراري

ناهدة بخيت حسن

آسيا حسين كاظم

قسم الفيزياء، كلية العلوم، جامعة بابل، العراق

### الكلمات المفتاحية:

أغشية أكسيد الحديد  
الرش الكيميائي الحراري  
الخصائص التركيبية  
الخصائص الطوبوغرافية

### الخلاصة:

تم بنجاح إضافة نسب تطعيم مختلفة (1، 3، 5٪) من ثاني أكسيد التيتانيوم TiO<sub>2</sub> إلى أغشية أكسيد الحديد النقية Fe<sub>2</sub>O<sub>3</sub> والمرسبة بطريقة الرش الكيميائي الحراري (SPT) على قواعد زجاجية. ودراسة تأثير التطعيم على الخصائص التركيبية والطوبوغرافية للأغشية الرقيقة المرسبة وذلك بواسطة تحليل حيود الأشعة السينية ومجهر القوى الذرية الـ (AFM) على التوالي. بينت نتائج الـ XRD أن جميع العينات متعددة التبلور وانخفاض الحجم البلوري مع زيادة نسبة الـ (TiO<sub>2</sub>). ظهرت لجميع الأغشية القمم (110)، (211)، (101)، (222)، (210)، (202)، (312)، (332)، (310) و (432) وبالالاتجاه المفضل (211). وظهرت نتائج الـ (AFM) أن الحجم الحبيبي ومعدل الخشونة ومربع الجذر التربيعي تقل بزيادة نسب التطعيم.

## 1. INTRODUCTION

Iron oxide exist in three stoichiometric forms namely magnetite ( $\text{Fe}_3\text{O}_4$ ), maghemite ( $\gamma\text{-Fe}_2\text{O}_3$ ) and hematite ( $\alpha\text{-Fe}_2\text{O}_3$ ) [1]. Recently, iron oxide  $\text{Fe}_2\text{O}_3$  is found to have large third-order non-linear optical susceptibility and faster response time showing potential applications in optical computing [2]. However, the device performance is related to the morphology, optical properties and structural order of the film, which in turn depend on the deposition technique and the growth parameters. Furthermore, the ferrite thin films exhibit an excellent magneto-optical property and also a strong chemical stability. Therefore, these films are suitable for magneto-optical memory and recording applications. On the other hand,  $\alpha\text{-Fe}_2\text{O}_3$  particles with various morphologies have been used widely as a raw material for the preparation of  $\alpha\text{-Fe}_2\text{O}_3$ , a useful magnetic recording material [3]. Many various materials of interest in spintronic as well as photovoltaic applications iron oxide is one of the most promising candidate [4]. Iron oxide films can be used in a wide range of applications. Iron oxide films can be used in a wide range of applications. Properties, such as high refractive index, wide band gap and chemical stability make iron oxide suitable for using as gas-sensors. The ferromagnetic films have many applications for microwave devices as well as high-density recording media [5]. In fact, hematite possesses semiconducting properties with an optical band gap of 2.1 eV and n-type were used in most applications. The concentration and the nature of charge carriers (electrons) are determined by the existence of oxide vacancies into the lattice. In particular conditions, it is possible to obtain also hematite of p-type as reported by *Y. Lin et al.*, [6], who succeeded in synthesis of p-type hematite via atomic layer deposition and Mg-doping [7].

Titanium dioxide  $\text{TiO}_2$  (titania) is a cheap, non-toxic and one of the most efficient semiconductor photocatalysts for extensive environmental applications because of its strong oxidizing power, high photochemical corrosive resistance and cost effectiveness. Due to these inherent properties,  $\text{TiO}_2$  is the most suitable candidate for degradation and complete mineralization of toxic organic pollutants in water [8].  $\text{TiO}_2$  has attracted much attention in

recent years due to its great potential for optical elements, electrical insulation, capacitors or gates in microelectronic devices, photovoltaic solar cells, anti-reflection coatings, optical waveguides and photonic crystals [9]. Researchers have employed several methods for depositing thin films like sol gel [10], chemical vapor deposition [11], magnetron sputtering [12], pulsed laser deposition [13], and spray pyrolysis [14]. Spray pyrolysis technique is frequently used because of its simplicity, commercial viability, potential for cost effective mass production, excellent control of chemical uniformity, and stoichiometry of thin films [15]. In this paper, the effect of doping with  $\text{TiO}_2$  has been studied on structural and morphological properties of  $\text{Fe}_2\text{O}_3$  thin films have been deposited by chemical spray pyrolysis before and after doping.

## 2. EXPERIMENTAL DETAILS

The basic principle involved in spray pyrolysis technique is pyrolytic decomposition of salts of a desired compound to be deposited. It mainly consists of spray nozzle, rotor for spray nozzle, liquid level monitor, hot plate, gas regulator valve and air tight fiber chamber. In spray pyrolysis, the process parameters like precursor solution, atomization of precursor solution, aerosol transport and decomposition of precursor are very important while studying the structural, optical, morphology and crystallinity of the thin films. Once the sprayed droplet reaching on the surface of the hot substrate undergoes pyrolytic decomposition and forms a single crystalline or cluster of crystallites as a final product. The other volatile by-products and solvents escape in the vapor phase. The substrates provide thermal energy for the thermal decomposition and subsequent recombination of the constituent species, followed by sintering and crystallization of the clusters of crystallites and thereby resulting in coherent film. The required thermal energy is different for the different materials and for the different solvents used in the spray process. The atomization of the spray solution into a spray of fine droplets also depends on the geometry of the spraying nozzle and pressure of a carrier gas. The film thickness depends upon the distance between the spray nozzle and substrate,

substrate temperature, concentration of the precursor solution and the quantity of the precursor solution sprayed [16].

TiO<sub>2</sub> doped ferric oxide (TiO<sub>2</sub>:Fe<sub>2</sub>O<sub>3</sub>) thin films were prepared onto glass substrates by using the chemical spray pyrolysis method. The solution was prepared by dissolving (FeCl<sub>3</sub>.9H<sub>2</sub>O) [purity 97.0%, Sinopharm Chemical Reagent Co., Ltd], it's molecular weight is (162.20) g.mol<sup>-1</sup> in distilled water. The concentrations of solution was 0.2 M and the color of the solution was reddish brown. The dissolving weight (Wt) of the materials were determined by using the following equation [17]:

$$M = (Wt / Mwt) \times (1000 / V) \dots\dots\dots (1)$$

Where M is the molar concentration, M<sub>wt</sub> is molecular weight and V is the volume of distilled water.

Also, TiO<sub>2</sub> be can prepared of titanium chloride (TiCl<sub>3</sub>) [AR grade, 99.9% pure, Merck made, Germany], it's molecular weight is (154.26) g.mol<sup>-1</sup>, in (50) mL distilled water at room temperature and using magnetic stirrer.

The TiO<sub>2</sub>:Fe<sub>2</sub>O<sub>3</sub> ratios calculated on in atomic percent (%) with starting solution of 1, 3 and 5 %. No additional additives or complexing agent is required to form the precursor solution. The precursor solution was sprayed onto the preheated glass substrates of [(7.5×2.5× 0.1) cm<sup>3</sup>] size with substrate temperature of 450 °C. While varying the doping percentage, other preparative parameters such as solution percentage (0.2 M), time of deposition is (4s) for each (1min). Restart spraying (20) times for each sample until the desired thickness of thin films is reached. The nozzle-to-substrate distance (30 cm) were kept constant for all experiments.

### 3. RESULTS AND DISCUSSION

#### A. Structural properties:

XRD patterns of deposited TiO<sub>2</sub>:Fe<sub>2</sub>O<sub>3</sub> thin films on glass substrate at different doping concentrations (0, 1, 3 and 5 %) were shown in Figures (1 to 4) in the range of 20°-80°. The presence of prominent diffraction peaks reveals to the polycrystalline nature of the films according to International Center for Diffraction

Data (ICDD) cards Number (96-101-1241). The interplanner spacing (d<sub>hkl</sub>) determined by using the Bragg relationship [18].

$$2d \sin\theta = n \lambda \dots\dots\dots (2)$$

where: n is an integer that indicates the order of the reflection, θ is Bragg diffraction angle of the XRD peak (degree); λ= 1.540600 Å is the wavelength of the X-ray beam .

The patterns show that all the thin films have peaks appears which be related to (110), (211), (101), (222), (210), (202), (312), (332), (310) and (432) planes at 2θ = 24.14, 33.14, 35.64, 39.24, 40.66, 49.45, 54.64, 57.45, 62.43 and 71.88 respectively of trigonal (rhombohedral axes) Fe<sub>2</sub>O<sub>3</sub> phase, they are having unit cell parameters (a= 5.4310 Å, α= 55.230°) in the hexagonal setting. This result agree with *J. Lee et al.*, [19]. Therefore, it can be concluded that all the films show high an intense diffraction peak (211) of Fe<sub>2</sub>O<sub>3</sub>. For all films, the crystallite size was calculated from the full width at half maximum (FWHM) (β) of the preferred orientation diffraction peak by using the Debye-Sherre's equation [20]:

$$D = k \lambda / (\beta \cos \theta) \dots\dots\dots (3)$$

Where: D is the crystallite size, k represents the shape factor, the value of which depends on the crystalline shape.

Figures (1 to 4) show the X-ray diffraction patterns of pure and TiO<sub>2</sub>:Fe<sub>2</sub>O<sub>3</sub> thin films deposited on glass substrates for various TiO<sub>2</sub> doping percentage. It is observed that no extra peaks of impurities other than the Fe<sub>2</sub>O<sub>3</sub> are observed even at high percentage content. Analyses of XRD diffractograms of TiO<sub>2</sub> doped Fe<sub>2</sub>O<sub>3</sub> have shown that samples contain only the hematite phase (rhombohedral), TiO<sub>2</sub> has been incorporated in the hematite crystal lattice, this result in agreement with *M. V. Nikolic et al.*, [21] and the intensity of peaks decreases with increasing doping percentage. This might be due to the incorporation of TiO<sub>2</sub> into the Fe<sub>2</sub>O<sub>3</sub> films which is able to create more defects in the lattice [22]. It can be seen in Figures (1 to 4) that with increase in TiO<sub>2</sub> content the peaks shift slightly to smaller angles.

From table (1) we can see a decrease in crystallite size from 23.120 nm to 17.307 nm when the TiO<sub>2</sub> % increased. The significant change in crystallite size which are due to

increase the reaction between the  $Fe_2O_3$  and  $TiO_2$ . As a result,  $TiO_2$  is likely to be easily trapped by  $Fe_2O_3$  and the average atoms mobility and diffusion length will decrease under high  $TiO_2$  %. Thus, the coalescence step will be not less kinetically limited, and resultant size of crystallite grains will smaller. During arriving particle to substrate, the particles suffer more collisions [23].

Also, to have more data on the measure of imperfections in the films, number of crystallite per unit surface area ( $N_\ell$ ), micro strain ( $\epsilon'$ ) and the dislocation density ( $\delta$ ), are evaluated in table (2) from equations (4), (5) and (6) respectively [24].

$$N_\ell = \frac{t}{D^3} \dots\dots\dots (4)$$

$$\epsilon' = \frac{\beta \cos\theta}{4} \dots\dots\dots (5)$$

$$\delta = \frac{1}{D^2} \dots\dots\dots (6)$$

From Table (2) dislocation density is the measure of amount of defects in a crystal and the values of micro strain and the dislocation density increase with increasing  $TiO_2$  % in the films, the micro strain depends directly on the lattice constant (c). While the number of crystallite per unit surface area decrease with increasing  $TiO_2$ .% in the films.

films.

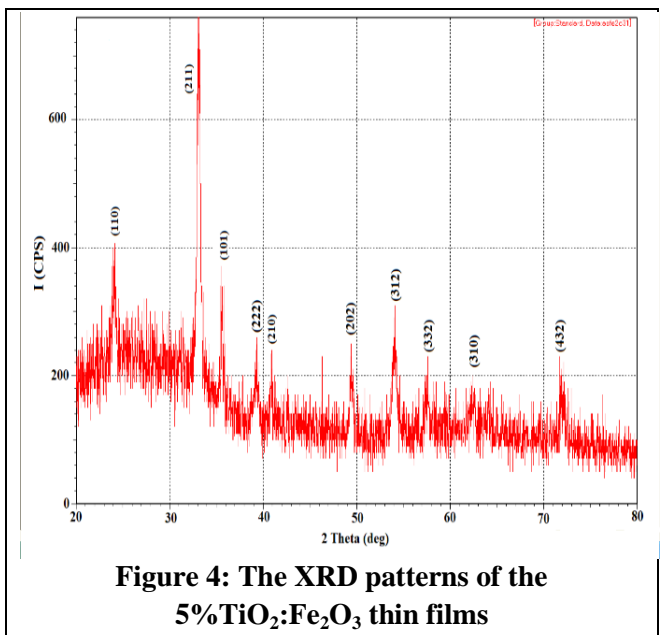
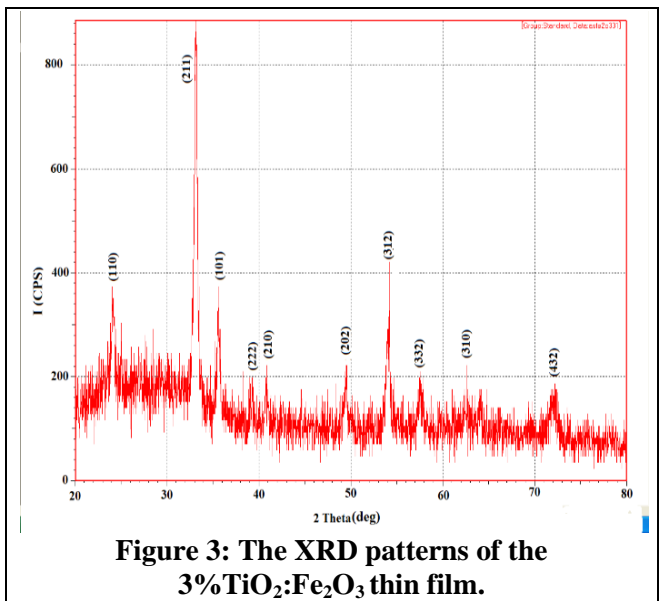
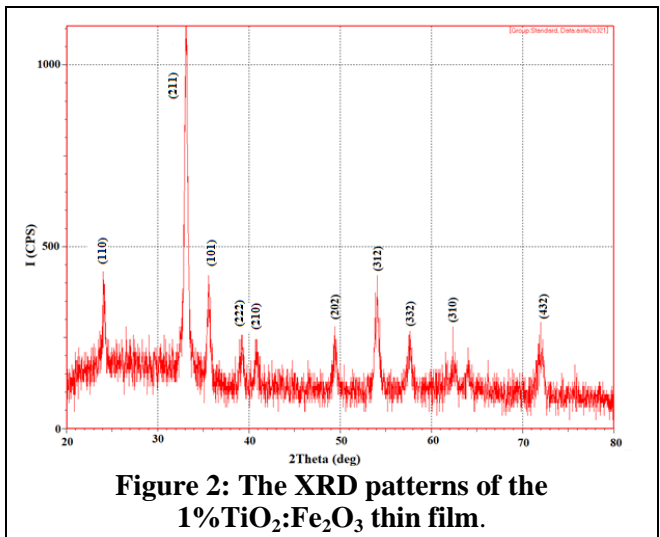
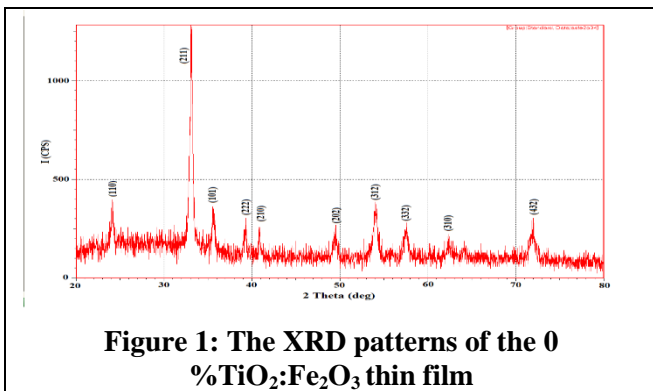


**Table (1): XRD parameters of pure Fe<sub>2</sub>O<sub>3</sub> and TiO<sub>2</sub>:Fe<sub>2</sub>O<sub>3</sub> thin films for preferred orientation (211).**

Sample	2θ (deg)	θ (deg)	d (nm)	FWHM (rad)	D <sub>av.</sub> (nm)
0 % TiO <sub>2</sub> :Fe <sub>2</sub> O <sub>3</sub>	33.14	16.57	0.270	0.006	23.601
1 % TiO <sub>2</sub> :Fe <sub>2</sub> O <sub>3</sub>	33.14	16.57	0.270	0.008	19.120
3 % TiO <sub>2</sub> :Fe <sub>2</sub> O <sub>3</sub>	33.13	16.565	0.271	0.008	18.543
5 % TiO <sub>2</sub> :Fe <sub>2</sub> O <sub>3</sub>	33.13	16.565	0.271	0.009	17.307

**Table (2): The number of layers (N<sub>av.</sub>), micro strain (ε<sub>av.</sub>) and the dislocation density (δ<sub>av.</sub>) for pure Fe<sub>2</sub>O<sub>3</sub> and TiO<sub>2</sub>:Fe<sub>2</sub>O<sub>3</sub> thin films for preferred orientation (211).**

Sample	ε <sub>av.</sub> × 10 <sup>-4</sup>	N <sub>av.</sub> × 10 <sup>16</sup> (m <sup>-2</sup> )	δ <sub>av.</sub> × 10 <sup>14</sup> (m <sup>-2</sup> )
0 % TiO <sub>2</sub> :Fe <sub>2</sub> O <sub>3</sub>	16.726	19.778	17.953
1 % TiO <sub>2</sub> :Fe <sub>2</sub> O <sub>3</sub>	18.116	37.195	27.353
3 % TiO <sub>2</sub> :Fe <sub>2</sub> O <sub>3</sub>	19.506	40.777	29.082
0 % TiO <sub>2</sub> :Fe <sub>2</sub> O <sub>3</sub>	22.310	50.154	33.385

**B. morphological Properties:**

AFM images of thin films prepared on glass substrate give the formation of the morphology properties. The pore average diameter, roughness average and root mean square have been estimated. The study of film surfaces is deposited important to recognize how the distribution and arrangement of atoms on surfaces, and get to know the differences or homogeneity properties or attributes relating to each atom separately.

Root mean square, roughness and grain size values were listed in Table (3). The average grain size of the particles is in nanoscale. Figure (5) show the AFM images were measured over an area of (900nm × 900nm). Figure (5 a, c, e, and g) shows the three-dimensional images of pure Fe<sub>2</sub>O<sub>3</sub> and TiO<sub>2</sub>:Fe<sub>2</sub>O<sub>3</sub> thin films it's found that surface thickness rats this value represents the thickness of the film surface roughness,

which account for the highest crystalline granular tops on the surface. Figure (5 b, d, f and h) shows the distribution of growth granular aggregates on the surface of the deposited films. The growth of small grains with increasing TiO<sub>2</sub> % leads to a decrease in the surface roughness. Table (3) shows the grain size of all thin film, one can observed that the grain size decreases with increasing of the doping ratios, this result agrees with (XRD) results and this lead to surface homogeneity. Also, the Table (3) shows the roughness for pure Fe<sub>2</sub>O<sub>3</sub> and TiO<sub>2</sub>:Fe<sub>2</sub>O<sub>3</sub> thin films and the root mean square (RMS) ( the sum of the highs and lows of surface squared divided by the sum of the total number under the square root ), where results decreases in roughness rate and the root mean square (RMS) with increasing the doping ratios it obvious that surface is smooth [25]

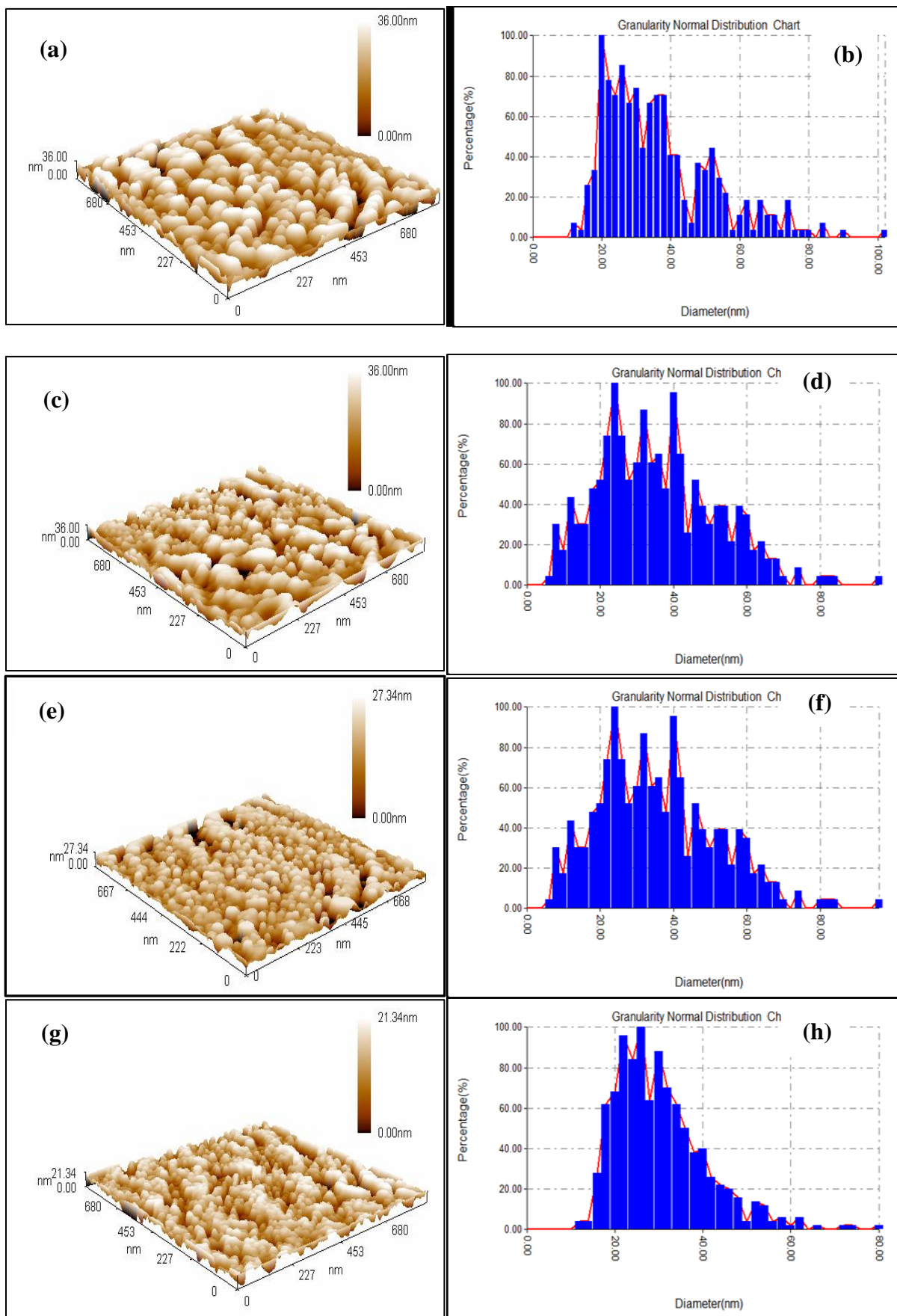


**Figure 5: 3-D analytical images and Granularity distribution for the prepared thin films: (a,b) 0 % TiO<sub>2</sub>:Fe<sub>2</sub>O<sub>3</sub>, (c,d) 1 % TiO<sub>2</sub>:Fe<sub>2</sub>O<sub>3</sub>, (e,f) 3 % TiO<sub>2</sub>:Fe<sub>2</sub>O<sub>3</sub>, (g,h) 5 % TiO<sub>2</sub>:Fe<sub>2</sub>O<sub>3</sub>.**

**Table 3: AFM parameters for pure Fe<sub>2</sub>O<sub>3</sub> and TiO<sub>2</sub>:Fe<sub>2</sub>O<sub>3</sub> thin films.**

Sample	RMS (nm)	Roughness (nm)	Grain Size (nm)
0 % TiO <sub>2</sub> :Fe <sub>2</sub> O <sub>3</sub>	9.93	8.48	35.56
1 % TiO <sub>2</sub> :Fe <sub>2</sub> O <sub>3</sub>	9.82	8.38	34.69
3 % TiO <sub>2</sub> :Fe <sub>2</sub> O <sub>3</sub>	6.94	5.79	34.02
5 % TiO <sub>2</sub> :Fe <sub>2</sub> O <sub>3</sub>	5.48	4.64	29.37

#### 4. CONCLUSION

Pure and doped Fe<sub>2</sub>O<sub>3</sub> thin films have been successfully deposited on glass substrates at 450 °C using spray pyrolysis technique. All films have polycrystalline and hematite phase (rhombohedral) with an average grain size of the particles decrease when the TiO<sub>2</sub> % increase. Calculated mean crystallite size of the selected planes of all thin films were found varying between (23.120 to 17.307) nm. The variation of crystallite size corroborates with XRD patterns and the growth of small grains with increasing TiO<sub>2</sub> % leads to a decrease in the surface roughness. Its observed that grain size decreases with increasing of the doping ratios, this result agree with XRD results. We can observe the roughness of thin films and the root mean square (RMS), where results decreases in roughness rate and the root mean square (RMS) with increasing the doping ratios it is obvious that surface is rough

#### 5. REFERENCES

- [1] A. Morisako, M. Matsumoto, M. Naoe, *IEEE Trans. Magn.* MAG-23 (1), p. 56, (1987).
- [2] M. Ando, K. Kandonno, M. Haruta, T. Sakaguchi, M. Miya, *Nature* 374, p. 625, (2002).
- [3] C.C. Chai, J. Peng, B.P. Yan, *Sens. Actuators B* 45, 49. (1997)
- [4] Yanagihara H., Myoka M., Isaka D., Niizeki, T., Mibu K. and Kita, "Selective growth of Fe<sub>3</sub>O<sub>4</sub> and γ-Fe<sub>2</sub>O<sub>3</sub> films with reactive magnetron sputtering", *J. Phys. D: Appl. Phys.*, 46, (2013).
- [5] R.C.Weast, and S.M.Selby, "Hand Book chemistry & physics", (CRC), 3rd edition, p.1245, (1967).
- [6] Y. Lin, Yang Xu, M. T. Mayer, Z. I. Simpson, G. M.Mahon, S. Zhou, and Dunwei Wang," Growth of p-Type Hematite by Atomic Layer Deposition and Its Utilization for Improved Solar Water Splitting", *J. Am. Chem. Soc.*, , 134 (12), pp. 5508–5511, (2012).
- [7] M. Congiu , M. L. De Marco , M. Bonomo , O. Nunes-Neto, D. Dini ,C. Graeff, " Pristine and Al-doped hematite printed films as photoanodes of p-type dye-sensitized solar cells", *J Nanopart Res*, pp.7-14, (2017).
- [8] M.O. Abou-Helal and W.T Seeber,. "Preparation of TiO<sub>2</sub> thin films by spray pyrolysis to be used as a photocatalyst." *Applied Surface Science*, p. 62, (2002).
- [9] R. Frua, H. Kawasaki, Harrison, G.W, Pamiko Wima." Preparation of high quality nitrogen doped TiO<sub>2</sub> thin film as a photocatalyst using a pulsed laser deposition method". *Thin Solid Films*, p.162, (2004).
- [10] H. Sun ,C. Cantalini, M. Faccio and M. Pelino," NO<sub>2</sub> gas sensitivity of sol-gel-derived α-Fe<sub>2</sub>O<sub>3</sub> thin films", *Volume 269*, pp. 97-101, (1995).
- [11] C. Hua, Y. Shang, Y. Wang, J. Xu, Y. Zhang, X. Li and A. Cao, "A flexible

- gas sensor based on single-walled carbon nanotube-Fe<sub>2</sub>O<sub>3</sub> composite film ", *Applied Surface Science* 405, pp. 405–411, (2017).
- [12] J. Krysa, M. Zlamal, S. Kment, M. Brunclikova and Z. Hubicka, "TiO<sub>2</sub> and Fe<sub>2</sub>O<sub>3</sub> films for photoelectrochemical water splitting", *Molecules* 20 (1), pp.1046-1058, (2015).
- [13] M. Yan, M. Lane, C. R. Kannewurf and R. P. H. Chang "Highly Conductive Epitaxial CdO Thin Films Prepared by Pulsed Laser Deposition", *Appl. Phys. Lett.* Vol.78 ,p 2342, (2001).
- [14] A. Akl, "Microstructure and electrical properties of iron oxide thin films deposited by spray pyrolysis", *Applied Surface Science* 221, pp. 319–329. (2004).
- [15] V.S. Mohite, M.A. Mahadik, S.S. Kumbhar, Y.M. Hunge, J.H. Kim, A.V. Moholkar, K.Y. Rajpure, C.H. Bhosale, " Photoelectrocatalytic degradation of benzoic acid using Au doped TiO<sub>2</sub> thin films", *Journal of Photochemistry and Photobiology B: Biology*, pp. 204–211,(2015).
- [16] P. S. Patil, "Versatility of chemical spray pyrolysis technique", *Mater. Chem. Phys.*, pp. 185–198, (1999).
- [17] H.A. Jassim, " Study the optical properties and electronic transition of the CdS and CdS:Cu thin films prepared by Spray Pyrolysis Technique", M.Sc. Thesis, university of Albasrah,(1989).
- [18] Y. Sirotnin and M. Shaskolskya, "Fundamental of Crystal Physics", Mir Pub., Moscow (1982).
- [19] J. Lee, Bhavana N. Joshi, J. Lee, T. Kim, Do-Yeon Kim, S. Al-Deyab, I. Seong, Mark T. Swihart, W. Yoon, S. Yoon, " Stable High-Capacity Lithium Ion Battery Anodes Produced by Supersonic Spray Deposition of Hematite Nanoparticles and Self-Healing Reduced Graphene Oxide", *Electrochimica Acta* 228, pp. 604–610, (2017).
- [20] J.C.Wilson, "X-Ray optics", London Methnen and coltd New York John,Wiley and SonsINC, pp. 1-5, (1962).
- [21] M. V. Nikolic, D. L. Sekulic, N. Nikolic, M. P. Slankamenac, O. S. Aleksic, H. Danninger, E. Halwax, V. B. Pavlovic, P. M. Nikolic, " Structural and Electrical Properties of Ti Doped  $\alpha$ -Fe<sub>2</sub>O<sub>3</sub>", *Science of Sintering*, pp. 281-292, (2013).
- [22] S.H. Park, J.H. Chang, H.J. Ko, T. Minegishi, J.S. Park, I.H. Im, M. Ito, D.C. Oh, M.W.Cho, T. Yao, "Lattice deformation of ZnO films with high nitrogen concentration,Appl", *Surf. Sci.* 254, pp. 7972–7975, (2008).
- [23] D. C. Monroy ,J. F. Ram," Effects of deposition parameters on the optical and microstructural characteristics of sputtered deposited nanocrystalline ZnO thin films ", *Revista Mexicana De Fisica* ,Vol. 53, No.5, pp.23–28,(2007).
- [24] Adel H. Alkhayatta and Shymaa K. Hussianb," Fluorine dopant concentration effect on the structural and optical properties of spray deposited nanocrystalline ZnO thin films", *Surfaces and Interfaces*, 8, pp.176–181, (2017).
- [25] G. Kadhim AL-Lamy," Fabrication and Study the Optoelectronics Properties of Detector NiO/c-Si by Spray Pyrolysis Technique", M.Sc.Thesis, Baghdad University, (2013).